PROCEEDINGS OF SPIE

SPIEDigitalLibrary.org/conference-proceedings-of-spie

Exact first order scattering correction for vector radiative transfer in coupled atmosphere and ocean systems

Peng-Wang Zhai, Yongxiang Hu, Damien Josset, Charles Trepte, Patricia Lucker, et al.

Peng-Wang Zhai, Yongxiang Hu, Damien B. Josset, Charles R. Trepte, Patricia L. Lucker, Bing Lin, "Exact first order scattering correction for vector radiative transfer in coupled atmosphere and ocean systems," Proc. SPIE 8364, Polarization: Measurement, Analysis, and Remote Sensing X, 83640A (8 June 2012); doi: 10.1117/12.920767

SPIE.

Event: SPIE Defense, Security, and Sensing, 2012, Baltimore, Maryland, United States

Exact first order scattering correction for vector radiative transfer in coupled atmosphere and ocean systems

Peng-Wang Zhai[a], Yongxiang Hu[b], Damien B. Josset[a], Charles R. Trepte[b], Patricia L. Lucker[a], and Bing Lin[b]

[a]SSAI 1 Enterprise Parkway Suite 200, Hampton, Virginia, 23666;
[b]NASA Langley Research Center, Hampton, VA 23681-2199.

ABSTRACT

We have developed a Vector Radiative Transfer (VRT) code for coupled atmosphere and ocean systems based on the successive order of scattering (SOS) method. In order to achieve efficiency and maintain accuracy, the scattering matrix is expanded in terms of the Wigner d functions and the delta fit or delta-M technique is used to truncate the commonly-present large forward scattering peak. To further improve the accuracy of the SOS code, we have implemented the analytical first order scattering treatment using the exact scattering matrix of the medium in the SOS code. The expansion and truncation techniques are kept for higher order scattering. The exact first order scattering correction was originally published by Nakajima and Takana.[1] A new contribution of this work is to account for the exact secondary light scattering caused by the light reflected by and transmitted through the rough air-sea interface.

Keywords: Atmospheric and ocean optics, Propagation, Radiative transfer, Scattering, Polarization

1. INTRODUCTION

Radiative transfer theory (RTT) has vast applications in astronomy, remote sensing, global climate modeling, and many other scientific disciplines.[2–4] The solution of radiative transfer equation (RTE) in a coupled atmosphere and ocean system (CAOS) is particularly important for ocean color remote sensing and interpretation of oceanographic field measurements. There are a number of radiative transfer solvers for a CAOS, for instance, using the methods of discrete ordinate,[5,6] matrix operator,[7–9] invariant embedding,[10] finite element,[11] and successive order of scattering (SOS),[12–15] iterative,[16] and Monte Carlo (MC).[17–20] The MC method is a special type in terms of its way of simulating photons propagating in turbid media stochastically. Many photon packages are initialized and launched in turbid media. The photons experience absorption and scattering events randomly. Detector responses are recorded either using estimation techniques or collecting photons which hits the detectors. Inherently, there is no space or angular discretization in the MC method. On the other hand, nearly all other methods in solving the RTE involve discretization of translational and/or angular spaces.

The radiance field in a turbid media is a function of viewing zenith and azimuth angles, space coordinates, and the inherent optical properties of scattering medium, and source conditions (external source like solar light or internal source like thermal emission). Discretization is a necessary way of representing the angular and space functional dependence in the deterministic solvers like the discrete ordinate methods. The azimuth angle dependence can be replaced by a Fourier number by expanding the radiance field into Fourier series. This will result in smaller memory requirements and shorter CPU time for most cases. The zenith angle is normally discretized by using Gaussian quadrature schemes. Accordingly, the scattering matrices of the turbid media are expanded in terms of the (associated) Legendre polynomials or equivalent expansion bases, with the number of expansion N_s bounded by the Gaussian quadrature numbers N_G to ensure numerical stability and accuracy.[21,22] In many cases, N_s is in the order of hundreds or even thousands mainly due to the large forward scattering peak in the scattering function. This in turn leads N_G to be unrealistically high because both the memory and CPU time depend on N_G nonlinearly.

To route the problem, the delta-M, δ-fit and other techniques are developed to truncate the forward peak of scattering function.[23,24] The basic idea is to approximate the narrow forward peak by Dirac delta function and

Send correspondence to Peng-Wang Zhai, E-mail: pengwang.zhai-1@nasa.gov.

Polarization: Measurement, Analysis, and Remote Sensing X
edited by David B. Chenault, Dennis H. Goldstein, Proc. of SPIE Vol. 8364, 83640A
 · doi: 10.1117/12.920767

rescale the optical depth and single scattering albedo to compensate the energy loss due to this approximation. The goal of these truncation techniques is to simulate the radiance field accurately by using moderate value of N_G at all viewing angles except the forward scattering lobe (for instance, solar aureole). Nakajima and Tanaka published a paper (hereafter refer to as NT88) showed that the simulation accuracy can be further improved by subtracting the single/double scattering contribution calculated with the truncated scattering function and adding back the corresponding single/double solution with the original exact scattering function.[1] NT88 technique successfully reduce the radiance relative error in every scattering region including the forward scattering lobe, which has been recognized as one of the 50 year milestone papers by Journal Of Quantitative Spectroscopy & Radiative Transfer (JQSRT).[25]

Besides the scattering function forward peak restoration, there are other cases that NT88 technique makes great sense. For instance, the scattering function of water clouds exhibits supernumerary bows for the scattering angle range of 140 to 170 degrees and catastrophic changes around the backscattering direction, if the effective variance of cloud particle size distribution is small (around 0.02). Brute force expansion of these scattering functions into Legendre polynomials takes hundreds/thousands of terms even after the truncation of the forward peak. NT88 technique can improve the radiance simulation in this case greatly as well. Nevertheless, NT88 still has some limitations as summarized by Ref. 22. One is that it neglects the surface reflection. In this paper, we extend the technique to include the case in which the specular surface reflection and transmission of the solar light source are treated as the primary light sources. Also polarization is treated exactly. In the next section, we will outline the theoretical formulas, which has been used to implement a computer code in the VRT code for the CAOS we developed based on the SOS method. Simulation examples and discussion will be Section 3 and summary will be given in Sec. 4.

2. THEORY

2.1 Radiative Transfer Equation

An integral form of the vector radiative transfer equation for a plane parallel medium without linear dichroism can be written as:[14]

$$\mathbf{L}(\tau,\mu<0,\phi) = \mathbf{L}(\tau_l,\mu,\phi)\exp\left(-\frac{\tau_l-\tau}{\mu}\right) - \int_{\tau_l}^{\tau}\exp\left(-\frac{\tau'-\tau}{\mu}\right)\mathbf{S}(\tau',\mu,\phi)\frac{d\tau'}{\mu}, \tag{1a}$$

$$\mathbf{L}(\tau,\mu>0,\phi) = \mathbf{L}(\tau_u,\mu,\phi)\exp\left(-\frac{\tau_u-\tau}{\mu}\right) + \int_{\tau}^{\tau_u}\exp\left(-\frac{\tau'-\tau}{\mu}\right)\mathbf{S}(\tau',\mu,\phi)\frac{d\tau'}{\mu}, \tag{1b}$$

where $\mathbf{L} = [I,Q,U,V]$ and I,Q,U,V are the Stokes parameters; τ is the optical depth along the vertical dimension; $\mu = \cos(\theta)$; θ and ϕ are the viewing zenith and azimuth angles, respectively; $\mu > 0$ denotes the upwelling direction and vice versa. τ_l and τ_u are the lower and upper optical depth limit of the scattering medium in consideration, respectively; $\mathbf{S}$ is the source function which accounts for the physical process of multiple scattering. In a macroscopically isotropic and mirror symmetric scattering medium and ignoring any internal source (thermal emission or fluorescence), the following expression is appropriate for the source function:

$$\mathbf{S}(\tau,\mu,\phi) = \frac{\omega(\tau)}{4\pi}\int_0^{2\pi}\int_{-1}^{1}\mathbf{P}(\tau,\mu,\phi,\mu',\phi')\cdot\mathbf{L}(\tau,\mu',\phi')d\mu'd\phi' + \mathbf{S}_1(\tau,\mu,\phi) \tag{2}$$

where ω is the single scattering albedo, $\mathbf{P} = \mathbf{R}(\pi-\chi_2)\cdot\mathbf{F}(\tau,\Theta)\cdot\mathbf{R}(-\chi_1)$ is the phase matrix;[2] $\mathbf{F}$ is the single scattering matrix of the medium and Θ is the scattering angle; $\mathbf{R}$ is the rotation matrix and χ_1 and χ_2 are the rotation angles, respectively; $\mathbf{S}_1$ is the source function due to the single scattering contribution. At the right hand side of Eq.(2), the first term represents the multiple scattering contribution of the source function. By separating the source function $\mathbf{S}$ into multiple and single scattering terms, the radiance vector $\mathbf{L}$ is now interpreted as the diffuse light which does not include the direct solar source beam.

The main purpose of this paper is to extend the NT88 technique to the CAOS. It is assumed that the atmosphere and ocean medium are separated by a flat ocean surface, as it is not possible to obtain a concise and simple analytical solution for secondary scattering light caused by the sun glint reflected from a wavy (rough) ocean surface. In this flat ocean case, the single scattering source function in the atmosphere includes two terms:

$$\mathbf{S}_1^a(\tau,\mu,\phi) = \mathbf{S}_1'(\tau,\mu,\phi) + \mathbf{S}_1''(\tau,\mu,\phi), \tag{3a}$$

$$\mathbf{S}_1'(\tau,\mu,\phi) = \frac{\omega(\tau)}{4\pi}\exp\left(\frac{\tau}{\mu_0}\right)\mathbf{P}(\tau,\mu,\phi,\mu_0,\phi_0)\cdot\mathbf{E}_0, \tag{3b}$$

$$\mathbf{S}_1''(\tau,\mu,\phi) = \frac{\omega(\tau)}{4\pi}\exp\left(\frac{2\tau_a^*-\tau}{\mu_0}\right)\mathbf{P}(\tau,\mu,\phi,-\mu_0,\phi_0)\cdot\mathbf{r}(\pi-\theta_0)\cdot\mathbf{E}_0, \tag{3c}$$

where $\mu_0 = \cos(\theta_0)$; θ_0 and ϕ_0 are the solar zenith and azimuth angles, respectively; τ_a^* is the optical depth just above the ocean surface; $\mathbf{r}$ is the Fresnel reflection matrix for the ocean surface; $\mathbf{E}_0 = [E_0, 0, 0, 0]$ and E_0 is the solar irradiance at the Top Of the Atmosphere (TOA). The first term $\mathbf{S}_1'(\tau,\mu,\phi)$ is the direct solar beam attenuated by the atmosphere while $\mathbf{S}_1''(\tau,\mu,\phi)$ is the Fresnel reflection of the solar light. It should be emphasized that Eqs. (3) only applies for $\tau < \tau_a^*$. Rigorously, $\mathbf{S}_1''(\tau,\mu,\phi)$ should be viewed as part of the second order scattering term, as the reflection itself is one order of interaction. We hypothetically treat it as part of the single scattering contribution because the Fresnel reflection is both physically and mathematically simple. The total radiance, in the end, is nevertheless correct regardless how we name an intermediate term. With the same logic we can write the single scattering source function in the ocean is caused by directly refracted solar light through the flat surface:[14]

$$\mathbf{S}_1^o(\tau,\mu,\phi) = \frac{\omega(\tau)}{4\pi}\left|\frac{\mu_0}{\mu_0'}\right|\exp\left(\frac{\tau-\tau_o}{\mu_0'}\right)\mathbf{P}(\tau,\mu,\phi,\mu_0',\phi_0)\cdot\mathbf{t}(\pi-\theta_0)\cdot\mathbf{E}_0\exp\left(\frac{\tau_a^*}{\mu_0}\right), \tag{4}$$

where $\mu_0' = \cos\theta_0'$, θ_0' is the angle of refraction for solar incident light determined by Snell's law: $\sin\theta_0 = n_w\theta_0'$, and n_w is the index of refraction for ocean water; τ_o is the optical depth just below the ocean surface and $\tau_o = \tau_a^* + \xi$ where ξ is an infinitesimal; and $\mathbf{t}$ is the Fresnel transmission matrix. Equation (4) is valid for $\tau > \tau_o$.

2.2 Analytical Single Scattering Solution

The single scattering solution to the VRTE can be obtained if the multiple scattering term in Eq. (2) is ignored. In other words, we can substitute Eqs.(3) and (4) into Eqs. (1) to find the single scattering solution for the atmosphere and ocean, respectively. In the atmosphere, we can write the single scattering solution $\mathbf{L}_1^a$ as:

$$\mathbf{L}_1^a = \mathbf{L}_1' + \mathbf{L}_1'', \tag{5a}$$

$$\mathbf{L}_1'(\tau,\mu<0,\phi) = -\int_0^{\tau}\exp\left(-\frac{\tau'-\tau}{\mu}\right)\mathbf{S}_1'(\tau',\mu,\phi)\frac{d\tau'}{\mu}, \tag{5b}$$

$$\mathbf{L}_1'(\tau,\mu>0,\phi) = \int_{\tau}^{\tau_a^*}\exp\left(-\frac{\tau'-\tau}{\mu}\right)\mathbf{S}_1'(\tau',\mu,\phi)\frac{d\tau'}{\mu}, \tag{5c}$$

$$\mathbf{L}_1''(\tau,\mu<0,\phi) = -\int_0^{\tau}\exp\left(-\frac{\tau'-\tau}{\mu}\right)\mathbf{S}_1''(\tau',\mu,\phi)\frac{d\tau'}{\mu}, \tag{5d}$$

$$\mathbf{L}_1''(\tau,\mu>0,\phi) = \int_{\tau}^{\tau_a^*}\exp\left(-\frac{\tau'-\tau}{\mu}\right)\mathbf{S}_1''(\tau',\mu,\phi)\frac{d\tau'}{\mu}, \tag{5e}$$

where $\tau_l = 0$ and $\tau_u = \tau_a^*$ are used for the atmosphere; and the boundary conditions $\mathbf{L}(\tau = 0,\mu,\phi)$ and $\mathbf{L}(\tau = \tau_a^*,\mu,\phi)$ are set to zeros as these are appropriate for the single scattering solution.

The radiance vector $\mathbf{L}_1'$ and $\mathbf{L}_1''$ can be explicitly evaluated using Eqs.(3) and (4). Generally, a vertically inhomogeneous atmosphere can be divided into a number of, say, N_L^a homogenous layers. The optical depth for the atmospheric layers can be denoted as $\tau_i, i = 0, 1, 2, ..., p, ..., N_L^a$, with $\tau_0 = 0$, $\tau_p = \tau$, $\tau_i < \tau_{i+1}$, and $\tau_{N_L^a} = \tau_a^*$.

$\mathbf{L}_1'$ can be written as:

$$\mathbf{L}_1'(\tau_p, \mu < 0, \phi) = -\sum_{i=0}^{p-1} \int_{\tau_i}^{\tau_{i+1}} \exp\left(-\frac{\tau' - \tau_p}{\mu}\right) \mathbf{S}_1'(\tau', \mu, \phi) \frac{d\tau'}{\mu}, \tag{6a}$$

$$= \mathbf{L}_1'(\tau_{p-1}, \mu < 0, \phi) \exp\left(-\frac{\tau_{p-1} - \tau_p}{\mu}\right) - \int_{\tau_{p-1}}^{\tau_p} \exp\left(-\frac{\tau' - \tau_p}{\mu}\right) \mathbf{S}_1'(\tau', \mu, \phi) \frac{d\tau'}{\mu}, \tag{6b}$$

$$= \mathbf{L}_1'(\tau_{p-1}, \mu < 0, \phi) \exp\left(-\frac{\tau_{p-1} - \tau_p}{\mu}\right) + \frac{\omega(\tau_p)}{4\pi} \frac{-\mu_0}{\mu - \mu_0} \left[\exp\left(\frac{\tau_p}{\mu_0}\right) - \exp\left(\frac{\tau_{p-1}}{\mu_0} - \frac{\tau_{p-1} - \tau_p}{\mu}\right)\right] \mathbf{P}(\tau_p, \mu, \phi, \mu_0, \phi_0) \cdot \mathbf{E}_0, \tag{6c}$$

where $\mathbf{P}(\tau, \mu, \phi, \mu_0, \phi_0)$ has been assumed to be invariant for $\tau_{p-1} < \tau_p$. Note that in the above equation the τ dependence of $\mathbf{L}_1'$ has been replaced by τ_p to obtain a recursive relation given by Eq.(6b) for inhomogeneous atmosphere layers. Eqs. (6) is equivalent to Eq. (65d) in Ref.22, except that we have replaced their summation over layers with a recursive relation for $\mathbf{L}_1'$, which is more convenient for numerical implementation. It should be understood that $\mathbf{L}_1'(\tau = 0, \mu < 0, \phi) = 0$ in using the recursive relation for $\mathbf{L}_1'$. Equation (6c) is singular for $\mu = \mu_0$. In this special case the solution reduces to:

$$\mathbf{L}_1'(\tau_p, \mu_0, \phi) = \mathbf{L}_1'(\tau_{p-1}, \mu_0, \phi) \exp\left(-\frac{\tau_{p-1} - \tau_p}{\mu_0}\right) + \frac{\omega(\tau_p)}{4\pi} \exp\left(\frac{\tau_p}{\mu_0}\right) \frac{\tau_p - \tau_{p-1}}{-\mu_0} \mathbf{P}(\tau_p, \mu_0, \phi, \mu_0, \phi_0) \cdot \mathbf{E}_0. \tag{7}$$

It should be emphasized again that $\mu_0 < 0$ is assumed in this paper since $\mu_0 = \cos\theta_0$ and $\theta_0 > \pi/2$. For $\mu > 0$, $\mathbf{L}_1'(\tau_p, \mu > 0, \phi)$ is:

$$\mathbf{L}_1'(\tau_p, \mu > 0, \phi) = \sum_{i=p}^{N_L^a - 1} \int_{\tau_i}^{\tau_{i+1}} \exp\left(-\frac{\tau' - \tau_p}{\mu}\right) \mathbf{S}_1'(\tau', \mu, \phi) \frac{d\tau'}{\mu}, \tag{8a}$$

$$= \mathbf{L}_1'(\tau_{p+1}, \mu > 0, \phi) \exp\left(-\frac{\tau_{p+1} - \tau_p}{\mu}\right) + \int_{\tau_p}^{\tau_{p+1}} \exp\left(-\frac{\tau' - \tau_p}{\mu}\right) \mathbf{S}_1'(\tau', \mu, \phi) \frac{d\tau'}{\mu}, \tag{8b}$$

$$= \mathbf{L}_1'(\tau_{p+1}, \mu > 0, \phi) \exp\left(-\frac{\tau_{p+1} - \tau_p}{\mu}\right) + \frac{\omega(\tau_p)}{4\pi} \frac{-\mu_0}{\mu - \mu_0} \left[\exp\left(\frac{\tau_p}{\mu_0}\right) - \exp\left(-\frac{\tau_{p+1} - \tau_p}{\mu} + \frac{\tau_{p+1}}{\mu_0}\right)\right] \mathbf{P}(\tau_p, \mu, \phi, \mu_0, \phi_0) \cdot \mathbf{E}_0, \tag{8c}$$

The radiance contribution $\mathbf{L}_1''$ can be evaluated in a way similar to $\mathbf{L}_1'$:

$$\mathbf{L}_1''(\tau_p, \mu < 0, \phi) = -\sum_{i=0}^{p-1} \int_{\tau_i}^{\tau_{i+1}} \exp\left(-\frac{\tau' - \tau_p}{\mu}\right) \mathbf{S}_1''(\tau', \mu, \phi) \frac{d\tau'}{\mu}, \tag{9a}$$

$$= \mathbf{L}_1''(\tau_{p-1}, \mu < 0, \phi) \exp\left(-\frac{\tau_{p-1} - \tau_p}{\mu}\right) - \int_{\tau_{p-1}}^{\tau_p} \exp\left(-\frac{\tau' - \tau_p}{\mu}\right) \mathbf{S}_1''(\tau', \mu, \phi) \frac{d\tau'}{\mu}, \tag{9b}$$

$$= \mathbf{L}_1''(\tau_{p-1}, \mu < 0, \phi) \exp\left(-\frac{\tau_{p-1} - \tau_p}{\mu}\right) + \frac{\omega(\tau_p)}{4\pi} \frac{\mu_0}{\mu + \mu_0} \exp\left(\frac{2\tau_a^* - \tau_p}{\mu_0}\right) \cdot \left\{1 - \exp\left[-(\tau_{p-1} - \tau_p)\left(\frac{1}{\mu_0} + \frac{1}{\mu}\right)\right]\right\} \mathbf{P}(\tau_p, \mu, \phi, -\mu_0, \phi_0) \cdot \mathbf{r}(\pi - \theta_0) \cdot \mathbf{E}_0, \tag{9c}$$

$$\mathbf{L}_1''(\tau_p,\mu>0,\phi) = \sum_{i=p}^{N_L^a-1}\int_{\tau_i}^{\tau_{i+1}} \exp\left(-\frac{\tau'-\tau_p}{\mu}\right)\mathbf{S}_1''(\tau',\mu,\phi)\frac{d\tau'}{\mu}, \tag{10a}$$

$$=\mathbf{L}_1''(\tau_{p+1},\mu>0,\phi)\exp\left(-\frac{\tau_{p+1}-\tau_p}{\mu}\right) + \int_{\tau_p}^{\tau_{p+1}} \exp\left(-\frac{\tau'-\tau_p}{\mu}\right)\mathbf{S}_1''(\tau',\mu,\phi)\frac{d\tau'}{\mu}, \tag{10b}$$

$$\begin{aligned}=&\mathbf{L}_1''(\tau_{p+1},\mu>0,\phi)\exp\left(-\frac{\tau_{p+1}-\tau_p}{\mu}\right) + \frac{\omega(\tau_p)}{4\pi}\frac{-\mu_0}{\mu+\mu_0}\exp\left(\frac{2\tau_a^*-\tau_p}{\mu_0}\right)\cdot\\ &\left\{\exp\left[-(\tau_{p+1}-\tau_p)\left(\frac{1}{\mu}+\frac{1}{\mu_0}\right)\right]-1\right\}\mathbf{P}(\tau_p,\mu,\phi,-\mu_0,\phi_0)\cdot\mathbf{r}(\pi-\theta_0)\cdot\mathbf{E}_0.\end{aligned} \tag{10c}$$

In case of $\mu+\mu_0=0$, $\mathbf{L}_1''(\tau_p,\mu>0,\phi)$ reduces to the form of:

$$\begin{aligned}\mathbf{L}_1''(\tau_p,-\mu_0,\phi) =&\mathbf{L}_1''(\tau_{p+1},-\mu_0,\phi)\exp\left(\frac{\tau_{p+1}-\tau_p}{\mu_0}\right)+\\ &\frac{\omega(\tau_p)}{4\pi}\frac{\tau_{p+1}-\tau_p}{-\mu_0}\exp\left(\frac{2\tau_a^*-\tau_p}{\mu_0}\right)\mathbf{P}(\tau_p,\mu,\phi,-\mu_0,\phi_0)\cdot\mathbf{r}(\pi-\theta_0)\cdot\mathbf{E}_0.\end{aligned} \tag{11}$$

The single scattering solution in the ocean $\mathbf{L}_1^o$ is:

$$\mathbf{L}_1^o(\tau,\mu<0,\phi) = -\int_{\tau_o}^{\tau}\exp\left(-\frac{\tau'-\tau}{\mu}\right)\mathbf{S}_1^o(\tau',\mu,\phi)\frac{d\tau'}{\mu}, \tag{12a}$$

$$\mathbf{L}_1^o(\tau,\mu>0,\phi) = \int_{\tau}^{\tau_o^*}\exp\left(-\frac{\tau'-\tau}{\mu}\right)\mathbf{S}_1^o(\tau',\mu,\phi)\frac{d\tau'}{\mu}, \tag{12b}$$

$$\tag{12c}$$

where $\tau_l=\tau_o$ and $\tau_u=\tau_o^*$ have been applied as τ_o^* is the optical depth at the ocean bottom; and the boundary conditions are set to zeros. Equations (12) can be evaluated analytically for a vertically inhomogeneous ocean body. The inhomogeneous ocean may be divided into N_L^o layers, and the inherent optical properties within each layer is homogenous. The optical depth in the ocean is denoted as $\tau_i, i=N_L^a+1, N_L^a+2, ..., p, ..., N_L^a+N_L^o+1$, with $\tau_{N_L^a+1}=\tau_o$, $\tau_p=\tau$, $\tau_{N_L^a+N_L^o+1}=\tau_o^*$, and $\tau_i<\tau_{i+1}$ assumed. Therefore, Equations (12) can be further developed into the following form:

$$\mathbf{L}_1^o(\tau_p,\mu<0,\phi) = -\sum_{i=N_L^a+1}^{p-1}\int_{\tau_i}^{\tau_{i+1}}\exp\left(-\frac{\tau'-\tau_p}{\mu}\right)\mathbf{S}_1^o(\tau',\mu,\phi)\frac{d\tau'}{\mu}, \tag{13a}$$

$$=\mathbf{L}_1^o(\tau_{p-1},\mu<0,\phi)\exp\left(-\frac{\tau_{p-1}-\tau_p}{\mu}\right) - \int_{\tau_{p-1}}^{\tau_p}\exp\left(-\frac{\tau'-\tau_p}{\mu}\right)\mathbf{S}_1^o(\tau',\mu,\phi)\frac{d\tau'}{\mu}, \tag{13b}$$

$$\begin{aligned}=&\mathbf{L}_1^o(\tau_{p-1},\mu<0,\phi)\exp\left(-\frac{\tau_{p-1}-\tau_p}{\mu}\right) + \frac{\omega(\tau_p)}{4\pi}\frac{-\mu_0}{\mu-\mu_0'}\exp\left(\frac{\tau_a^*}{\mu_0}\right)\cdot\\ &\left[\exp\left(\frac{\tau_p-\tau_o}{\mu_0'}\right)-\exp\left(\frac{\tau_{p-1}-\tau_o}{\mu_0'}-\frac{\tau_{p-1}-\tau_p}{\mu}\right)\right]\mathbf{P}(\tau,\mu,\phi,\mu_0',\phi_0)\cdot\mathbf{t}(\pi-\theta_0)\cdot\mathbf{E}_0,\end{aligned} \tag{13c}$$

$$\begin{aligned}\mathbf{L}_1^o(\tau_p,\mu_0',\phi) =&\mathbf{L}_1^o(\tau_{p-1},\mu_0',\phi)\exp\left(-\frac{\tau_{p-1}-\tau_p}{\mu_0'}\right)+\\ &\frac{\omega(\tau_p)}{4\pi}\left|\frac{\mu_0}{\mu_0'}\right|\exp\left(\frac{\tau_a^*}{\mu_0}\right)\frac{\tau_{p-1}-\tau_p}{|\mu_0'|}\mathbf{P}(\tau,\mu,\phi,\mu_0',\phi_0)\cdot\mathbf{t}(\pi-\theta_0)\cdot\mathbf{E}_0,\end{aligned} \tag{14}$$

$$\mathbf{L}_1^o(\tau_p,\mu>0,\phi)=\sum_{i=p}^{N_L^a+N_L^o}\int_{\tau_i}^{\tau_{i+1}}\exp\left(-\frac{\tau'-\tau_p}{\mu}\right)\mathbf{S}_1^o(\tau',\mu,\phi)\frac{d\tau'}{\mu}, \tag{15a}$$

$$=\mathbf{L}_1^o(\tau_{p+1},\mu>0,\phi)\exp\left(-\frac{\tau_{p+1}-\tau_p}{\mu}\right)+\int_{\tau_p}^{\tau_{p+1}}\exp\left(-\frac{\tau'-\tau_p}{\mu}\right)\mathbf{S}_1^o(\tau',\mu,\phi)\frac{d\tau'}{\mu}, \tag{15b}$$

$$=\mathbf{L}_1^o(\tau_{p+1},\mu>0,\phi)\exp\left(-\frac{\tau_{p+1}-\tau_p}{\mu}\right)+\frac{\omega(\tau_p)}{4\pi}\frac{-\mu_0}{\mu-\mu_0'}\exp\left(\frac{\tau_a^*}{\mu_0}\right)\cdot$$
$$\left[\exp\left(\frac{\tau_p-\tau_o}{\mu_0'}\right)-\exp\left(\frac{\tau_{p+1}-\tau_o}{\mu_0'}-\frac{\tau_{p+1}-\tau_p}{\mu}\right)\right]\mathbf{P}(\tau,\mu,\phi,\mu_0',\phi_0)\cdot\mathbf{t}(\pi-\theta_0)\cdot\mathbf{E}_0, \tag{15c}$$

where Eq.(14) is a special case of Eq.(13) for $\mu=\mu_0'$.

2.3 Single Scattering Radiance Correction for CAOS

Equations (5a), (6c), (7), (8c),(9c),(10c), (11),(13c), (14), and (15c) forms a complete set of analytical single scattering solutions for VRTE in CAOS. In this section, we use these exact analytical solutions to correct the radiance field calculated by the SOS code following the procedure described in Ref.22. The scheme we adopt is the so-called TMS in NT88.[1] It is necessary to recall that the δ-M or delta-fit methods approximate the forward peak of the exact phase function $\mathbf{F}_{11}(\tau,\Theta)$ as a δ function:

$$\mathbf{F}_{11}(\tau,\Theta)\approx 2f\delta(1-\cos\Theta)+(1-f)\mathbf{F}'_{11}(\tau,\Theta), \tag{16}$$

where f is the fractional scattering energy within the truncated forward peak; and $\mathbf{F}'_{11}$ is the approximated phase function. To use $\mathbf{F}'_{11}$ to represent $\mathbf{F}_{11}$ in the RTE system, the optical thickness $d\tau$ and single scattering albedo ω have to be scaled:

$$d\tau'=(1-\omega f)d\tau, \tag{17a}$$

$$\omega'=\frac{1-f}{1-\omega f}\omega. \tag{17b}$$

If we use $\mathbf{L}'$ to denote the vector radiance field obtained by Eqs. (16) and (17), the NT88 TMS scheme is:

$$\mathbf{L}_{corrected}=\mathbf{L}'+\Delta\mathbf{L}_{TMS}, \tag{18a}$$

$$\Delta\mathbf{L}_{TMS}=\mathcal{L}\left[\frac{\omega\mathbf{F}_{11}}{1-\omega f},\tau'\right]-\mathcal{L}\left[\omega'\mathbf{F}'_{11},\tau'\right], \tag{18b}$$

where $\mathcal{L}$[phase function, optical depth] is a schematic notation for the single scattering solution for CAOS outlined in the previous section. We refer the readers to Ref.1 and 22 for the justification of this NT88 TMS scheme.

3. RESULTS AND DISCUSSION

The single scattering correction scheme for the CAOS outlined in Sec.2 is implemented in the vector radiative transfer solver based on the SOS method.[14,15] The validation of the model is done against another independent radiative transfer model based on the MC method.[20] A test case is designed to verify the implementation. The scenario includes both an atmosphere and ocean with equal optical depth of 0.5. The single scattering albedo for both the atmosphere and ocean is 0.99. The scattering matrix for both the atmosphere and ocean is the well known L=60 model introduced in Refs. 26, 27, which corresponds to the spherical particles of a gamma size distribution (see Eq. 5.245 in Ref. 28) with the effective radius of 1.05 μm and the effective variance of 0.07 and is for the wavelength of 0.782 μm and the refractive index of 1.43. The ocean surface is flat with refractive index of 1.338. The reflection of the ocean bottom is lambertian with a reflection albedo of 0.1. The solar source zenith angle is 78.4630° with Stokes parameters of $(\pi,0,0,0)$. The motivation of this unrealistically simplified case is to emphasize the interactive boundary condition of the atmosphere and ocean interface so that small errors due to any part of the code will be noticeable. The full Stokes parameters at four locations are calculated with both the SOS and MC methods: Top Of the Atmosphere (TOA), Bottom Of the Atmosphere (BOA), Top Of the Ocean (TOO), and Bottom Of the Ocean (BOO). In the MC method, a photon history of 5×10^6 is used to ensure statistical convergence. The SOS method used high Gaussian quadrature numbers of $N_G = 100$ (100 streams) and 200 in the atmosphere and ocean, respectively.

Figures 1, 2, 3, and 4 show the Stokes parameters as a function of viewing zenith angles at the four locations calculated by both methods. All the subfigures share the same plot marker symbols. Three viewing azimuth angles are shown: $\phi = 0, 90°$ and $180°$. The agreements for all four Stokes parameters between the SOS and MC methods are excellent for all viewing angles at all four locations. The maximum percentage difference between the two methods are smaller than 0.1% percents (not shown) for all locations and angles. Hereafter the SOS results shown in Figs. 1, 2, 3, and 4 are regarded as the "true" solution to the test case due to the unambiguous agreements between two independent methods. Specifically, the radiances are smooth at the TOA with respect to the viewing zenith angles, but show rather abrupt changes for all other locations. At the TOO, the radiances are nearly symmetrical around viewing angle of 90° due to the total reflection. At the critical angle of $180 - asin(1.0/1.338) = 131.6357°$, the radiance is discontinues because the atmospheric radiance transmission. At the BOO, the radiances show similar features but with smaller magnitude. The circular polarization components V/I for all locations are small but not negligible.

The single scattering correction scheme is useful in a sense that it should improve the simulation accuracy for smaller and insufficient number of streams. Therefore the calculation in Figs. 1, 2, 3, and 4 are repeated with $N_G = 30$ in the atmosphere ($N_G = 60$ in the ocean), with and without the single scattering correction scheme. Figure 5 shows the percentage error of the SOS radiances for $N_G = 30$ without the single scattering correction, using the case of $N_G = 100$ as the benchmark. Figure 6 is the same as Fig. 5 but with the single scattering correction. The relative errors of the radiance at the TOA are smaller than 0.5% for viewing zenith angles smaller than 60%, with or without the correction, but increase to 3% for larger viewing zenith angles if no single scattering correction is used. The single scattering correction decreases the relative errors at the TOA, especially for viewing zenith angles larger than 60°. For the BOA, the single scattering correction improves the results for $\phi = 90°$ and $180°$, but not for $\phi = 0°$. This is because the radiance field for $\phi = 0°$ is rapidly changing around the forward scattering direction (see Fig. 2). The SOS model only calculates the radiance field at the Gaussian quadrature angles. A polynomial interpolation is used to obtain the radiances at arbitrary output angles. In the case of non-smooth radiance field, the interpolation error dominates the error introduced by the phase matrix approximation used in the calculation. Thus the single scattering correction does not help much. For the same reason, the single correction scheme does not improve the accuracy of the radiance fields at the TOO and BOO. In order to improve the simulation for cases of non-smooth radiance field, a better interpolation scheme is desired. We have developed an advanced interpolation scheme based on the technique in Ref. 29, which improves the accuracy a lot. However, the detailed discussion of the interpolation scheme is out of the scope of this paper. We will prepare and submit a separate paper to discuss the usage of that interpolation technique in the CAOS.

4. SUMMARY

In this paper the single scattering correction technique is extended to the CAOS and implemented in the vector radiative transfer code based on the SOS method. The Stokes parameter as a function of the viewing angles are calculated for a test case for the TOA, BOA, TOO, and BOO. Two independent methods, the SOS and MC methods, are used to calculate the polarized radiance field. For a sufficiently high number of Gaussian quadrature points, the agreement of the SOS and MC results is excellent (percentage error smaller than 0.1% for all locations and viewing angles). If the Gaussian quadrature number is not large enough, the accuracy of the SOS method decrease. If the radiance field is smooth with respect to the viewing zenith angle, the single scattering correction scheme improve the accuracy from 3% to within 1%. On the other hands, single scattering correction does not help much for a non-smooth radiance field as the interpolation errors dominate.

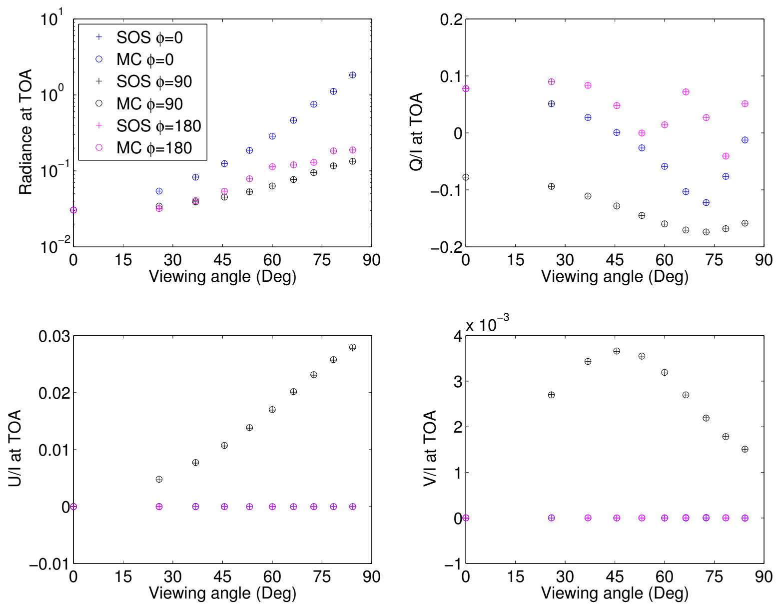

Figure 1. Stokes parameters at the TOA.

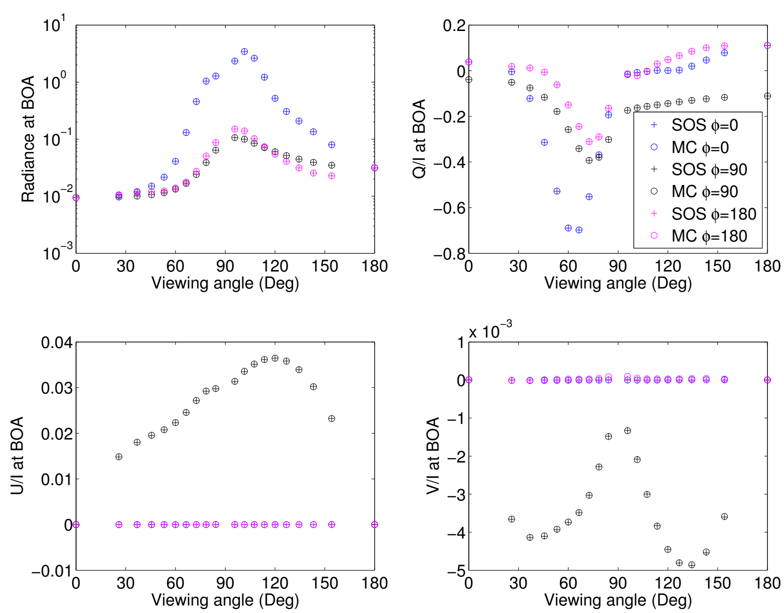

Figure 2. Stokes parameters at the BOA.

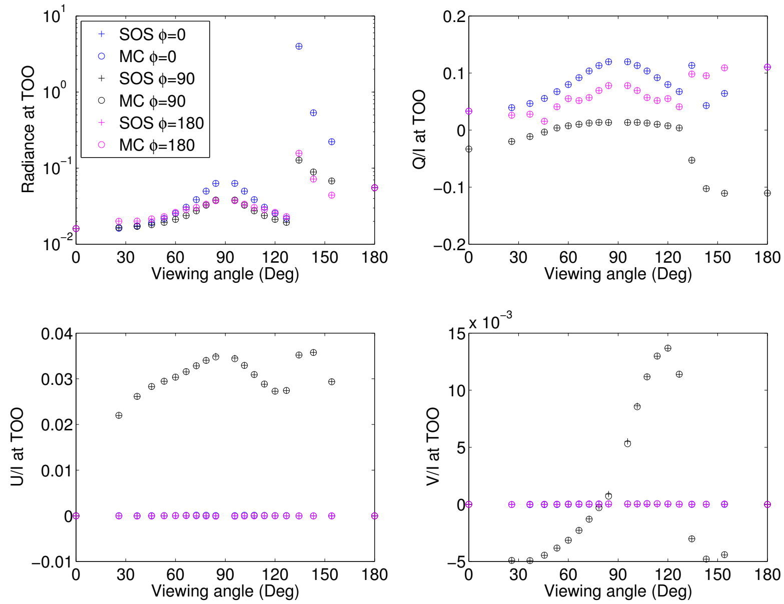

Figure 3. Stokes parameters at the TOO.

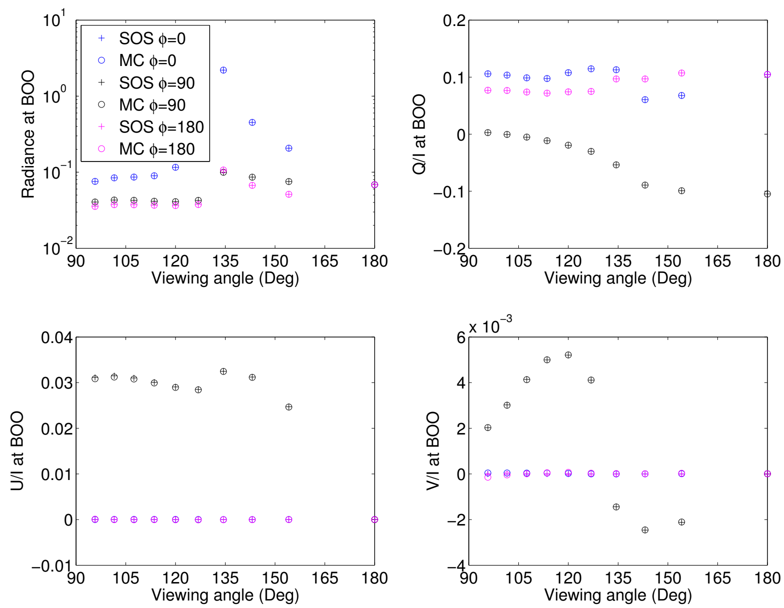

Figure 4. Stokes parameters at the BOO.

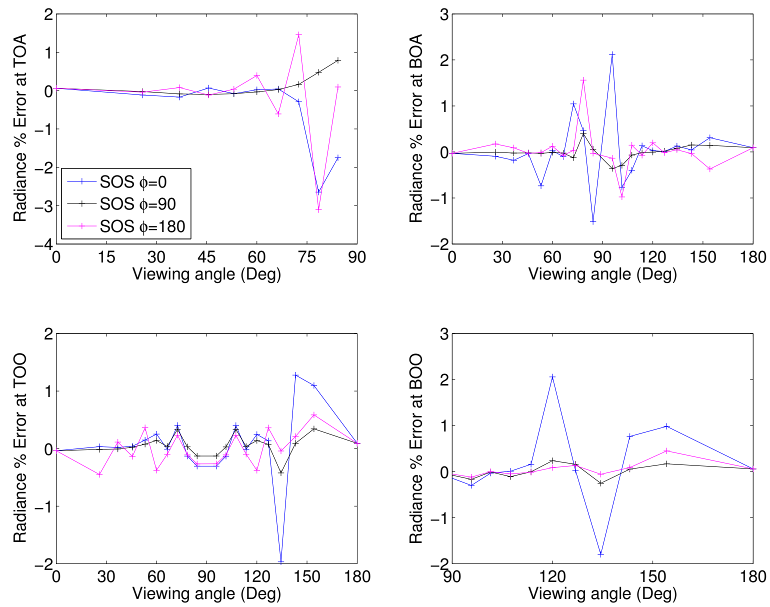

Figure 5. Radiance Percentage Error for N_G=30 without the single scattering correction.

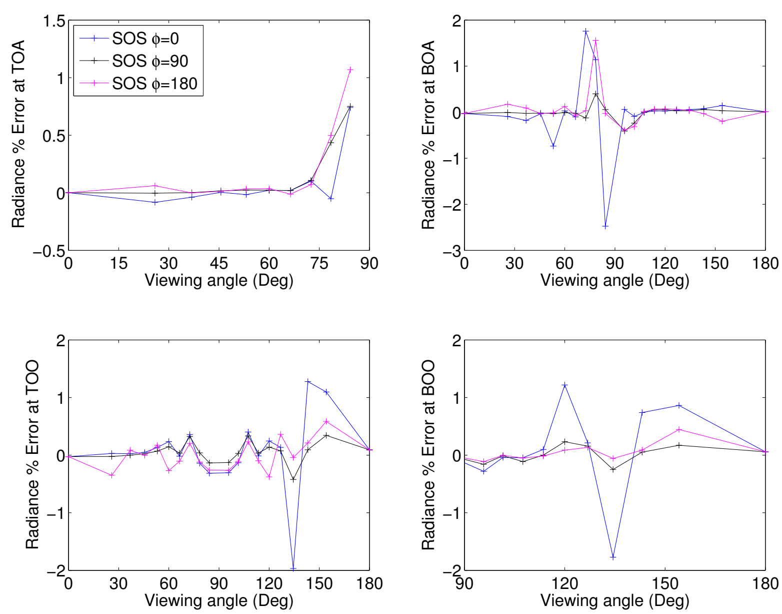

Figure 6. Radiance Percentage Error for N_G=30 with the single scattering correction.

ACKNOWLEDGMENTS

This study is supported by the NASA Radiation Science program administrated Hal Maring and the Biogeochemistry program administrated by Paula Bontempi.

REFERENCES

[1] Nakajima, T. and Tanaka, M., "Algorithms for radiative intensity calculations in moderately thick atmospheres using a truncation approximation," *J. Quant. Spectrosc. Radiat. Transfer* **40**, 51–69 (1988).

[2] Chandrasekhar, S., [*Radiative transfer*], Dover, New York (1960).

[3] Liou, K., [*An Introduction to Atmospheric Radiation*], Academic Press, San Diego (2002 (second edition)).

[4] Mishchenko, M. I., Travis, L. D., and Lacis, A. A., [*Multiple Scattering of Light by Particles: Radiative Transfer and Coherent Backscattering*], Cambridge University Press, Cambridge (2006).

[5] Jin, Z. and Stamnes, K., "Radiative transfer in nonuniformly refracting layered media: atmosphere-ocean system," *Appl. Opt.* **33**, 431–442 (1994).

[6] Jin, Z., Charlock, T. P., Rutledge, K., Stamnes, K., and Wang, Y., "Analytical solution of radiative transfer in the coupled atmosphereocean system with a rough surface," *Appl. Opt.* **45**, 7443–7455 (2006).

[7] Nakajima, T. and Tanaka, M., "Effect of wind-generated waves on the transfer of solar radiation in the atmosphere-ocean system," *J. Quant. Spectrosc. Radiat. Transfer* **29**, 521–537 (1983).

[8] Fischer, J. and Grassl, H., "Radiative transfer in an atmosphere-ocean system: an azimuthally dependent matrix operator approach," *Appl. Opt.* **23**, 1032–1039 (1984).

[9] Chowdhary, J., Cairns, B., and Travis, L. D., "Contribution of water-leaving radiances to multiangle, multispectral polarimetric observations over the open ocean: bio-optical model results for case 1 waters," *Appl. Opt.* **45**, 5542–5567 (2006).

[10] Mobley, C. D., Gentili, B., Gordon, H. R., Jin, Z., Kattawar, G. W., Morel, A., Reinersman, P., Stamnes, K., and Stavn, R. H., "Comparison of numerical models for computing underwater light fields," *Appl. Opt.* **32**, 7484–7504 (1993).

[11] Bulgarelli, B., Kisselev, V. B., and Roberti, L., "Radiative transfer in the atmosphere-ocean system: The finite-element method," *Appl. Opt.* **38**, 1530–1542 (1999).

[12] Gordon, H. and WANG, M., "Surface-roughness considerations for atmospheric correction of ocean color sensors .1. the Rayleigh-scattering component," *Appl. Opt.* **31**, 4247–4260 (JUL 20 1992).

[13] Chami, M., Santer, R., and Dilligeard, E., "Radiative transfer model for the computation of radiance and polarization in an ocean-atmosphere system: polarization properties of suspended matter for remote sensing," *Appl. Opt.* **40**, 2398–2416 (2001).

[14] Zhai, P.-W., Hu, Y., Trepte, C. R., and Lucker, P. L., "A vector radiative transfer model for coupled atmosphere and ocean systems based on successive order of scattering method," *Opt. Express* **17**, 2057–2079 (FEB 16 2009).

[15] Zhai, P.-W., Hu, Y., Chowdhary, J., Trepte, C. R., Lucker, P. L., and Josset, D. B., "A vector radiative transfer model for coupled atmosphere and ocean systems with a rough interface," *J. Quant. Spectrosc. Radiat. Transfer* **111**, 1025–1040 (MAY 2010).

[16] Ahmad, Z. and Fraser, R. S., "An Iterative Radiative Transfer Code For Ocean-Atmosphere Systems.," *Journal of Atmospheric Sciences* **39**, 656–665 (Mar. 1982).

[17] Kattawar, G. W. and Adams, C. N., "Stokes vector calculations of the submarine light field in an atmosphere-ocean with scattering according to a rayleigh phase matrix: effect of interface refractive index on radiance and polarization," *Limnol. Oceanogr.* **34**, 1453–1472 (1989).

[18] Tynes, H. H., Kattawar, G. W., Zege, E. P., Katsev, I. L., Prikhach, A. S., and Chaikovskaya, L. I., "Monte carlo and multicomponent approximation methods for vector radiative transfer by use of effective mueller matrix calculations," *Appl. Opt.* **40**, 400–412 (2001).

[19] Gray, D. J., Kattawar, G. W., and Fry, E. S., "Design and analysis of a flow-through integrating cavity absorption meter," *Appl. Opt.* **45**, 8990–8998 (DEC 10 2006).

[20] Zhai, P., Kattawar, G. W., and Yang, P., "Impulse response solution to the three-dimensional vector radiative transfer equation in atmosphere-ocean systems. i. monte carlo method," *Appl. Opt.* **47**, 1037–1047 (2008).

[21] Stamnes, K., Tsay, S.-C., Wiscombe, W., and Jayaweera, K., "Numerically stable algorithm for discrete-ordinate method radiative trasfer in multiple scattering and emitting layered media," *Appl. Opt.* **27**, 2502–2509 (1988).

[22] Stamnes, K., Tsay, S.-C., Wiscombe, W., and Laszlo, I., "A general-purpose numerically stable computer code for discrete-ordinate-method radiative transfer in scattering and emitting layered media," *DISORT Report v1.1* (2000).

[23] Wiscombe, W. J., "The delta-m method: rapid yet accurate radiative flux calculations for strongly asymmetric phase functions," *J. Atmos. Sci.* **34**, 1408–1422 (1977).

[24] Hu, Y. X., Wielicki, B., Lin, B., Gibson, G., Tsay, S. C., Stamnes, K., and Wong, T., "δ-fit: A fast and accurate treatment of particle scattering phase functions with weighted singular-value decomposition least-squares fitting," *J. Quant. Spectrosc. Radiat. Transfer* **65**, 681–690 (2000).

[25] Mishchenko, M. I., Rothman, L. S., Mengçü, M. P., and Stoop, J., "50 years of jqsrt: Milestone papers," *J. Quant. Spectrosc. Radiat. Transfer* **111**(11), 1455 – 1458 (2010). 50 Years of JQSRT.

[26] Vestrucci, P. and Siewert, C., "A numerical evaluation of an analytical representation of the components in fourier decomposition of the phase matrix for the scattering of the polarized light," *J. Quant. Spectrosc. Radiat. Transfer* **31**, 177–183 (1984).

[27] Garcia, R. and Siewert, C., "A generalized spherical harmonics solution for radiative transfer models that include polarization effects," *J. Quant. Spectrosc. Radiat. Transfer* **36**, 401–423 (1986).

[28] Mishchenko, M., Travis, L., and Lacis, A., [*Scattering, Absorption, and Emission of Light by Small particles*], Cambridge University Press, Cambridge (2002).

[29] Schulz, F. and K.Stamnes, "Angular distribution of the stokes vector in a plane-parallel vertically inhomogeneous medium in the vector discrete ordinate radiative transfer (vdisort) model," *J. Quant. Spectrosc. Radiat. Transfer* **65**, 609–620 (2000).